Letter

Scanning ultrafast electron microscopy reveals photovoltage dynamics at a deeply buried *p*-Si/SiO₂ interface

S. R. Ellis,[1] N. C. Bartelt,[1] F. Léonard,[1] K. C. Celio,[1] E. J. Fuller,[1] D. R. Hughart,[2] D. Garland,[2]
M. J. Marinella,[2] J. R. Michael,[2] D. W. Chandler,[1] B. Liao,[3] and A. A. Talin[1,*]

[1]*Sandia National Laboratories, Livermore, California 94550, USA*
[2]*Sandia National Laboratories, Albuquerque, New Mexico 87185, USA*
[3]*Department of Mechanical Engineering, University of California, Santa Barbara, California 93106, USA*

The understanding and control of charge carrier interactions with defects at buried insulator/semiconductor interfaces is essential for achieving optimum performance in modern electronics. Here, we report on the use of scanning ultrafast electron microscopy (SUEM) to remotely probe the dynamics of excited carriers at a Si surface buried below a thick thermal oxide. Our measurements illustrate a previously unidentified SUEM contrast mechanism, whereby optical modulation of the space-charge field in the semiconductor modulates the electric field in the thick oxide, thus affecting its secondary electron yield. By analyzing the SUEM contrast as a function of time and laser fluence we demonstrate the diffusion mediated capture of excited carriers by interfacial traps.

I. INTRODUCTION

The understanding and control of electric fields and charge flow at interfaces is critical to the improvement of modern electronic and optoelectronic devices. However, nondestructive interface characterization techniques with nanometer spatial resolution such as electron beam induced current (EBIC) [1] or ballistic electron emission microscopy (BEEM) [2] generally operate at or near DC timescales, while techniques with high temporal resolution such as optical pump-probe spectroscopy generally have poor spatial resolution. These limitations pose a challenge to semiconductor material and device characterization since important processes such as interface carrier recombination occur at subnanosecond timescales and critical dimensions of modern devices are in the few-nanometer regime. Scanning ultrafast electron microscopy (SUEM) is a nascent technique that aims to combine the nanometer spatial resolution of a scanning electron microscope (SEM) with the temporal resolution of ultrafast lasers, enabling investigations of ultrafast dynamics well below the optical diffraction limit [3–5].

As shown schematically in Fig. 1, SUEM operates on a stroboscopic principle. A pulsed optical laser (pump) excites a sample while a pulsed electron beam (probe) inspects the dynamics at given time delays with respect to the pump. The probe is tightly focused and scanned across the sample, generating a secondary electron (SE) contrast image at each time delay, which collectively forms an ultrafast SEM movie of the pump-induced dynamics. Ultrafast SUEM movies have revealed surprising charge carrier dynamics in simple systems, including ballistic transport at Si *p-n* junctions [6], superdiffusion of photoexcited carriers in *p*- and *n*-type Si [7],

spontaneous separation of photoexcited electrons and holes in hydrogenated amorphous silicon [8], and anisotropic photo-carrier diffusion in black phosphorus [9].

Herein we demonstrate that SUEM can probe electric fields and ultrafast charge recombination dynamics at deeply buried interfaces well beyond the escape depth of secondary electrons. Specifically, we show that transient photovoltage (PV) at a *p*-Si/SiO₂ interface, produced by photoexcitation and subsequent trapping of minority carriers, modulate the secondary electron (SE) emissions originating from the surface region of a 1 μm thick oxide (Fig. 1).

II. METHODS

The SUEM setup consists of a 532 nm Fianium HYLASE fiber laser (2 MHz repetition rate, 10 ps pulses) that is coupled to a Philips/FEI XL30s SEM through windows in the SEM chamber and in the field emission gun. The 10 ps electron beam pulses are generated by focusing 50 nJ of the 355 nm laser light (third harmonic) onto the apex of the ZrO/W Schottky field emitter. A 200 μm electron beam aperture results in an average electron beam current of ∼1 pA (three electrons per pulse) at the sample. The 532 nm light from the laser is time delayed through a variable optical path and focused on the sample (focal length = 200 mm) with an angle of incidence of 66° to generate the pump beam. To minimize noise induced by instability in the probe, the pump laser is modulated in a shot to shot fashion at 1 MHz by an electro-optic modulator (EOM, Con-Optics M370 LA 25A) with a 70:1 attenuation.

The SEs are detected with a microchannel plate (MCP) detector, which offers better light rejection than that of an Everhart-Thornley detector. The SEs are directed toward the MCP with a +300 V bias applied to the front of the MCP and a −300 V bias applied to the sample mount. The current
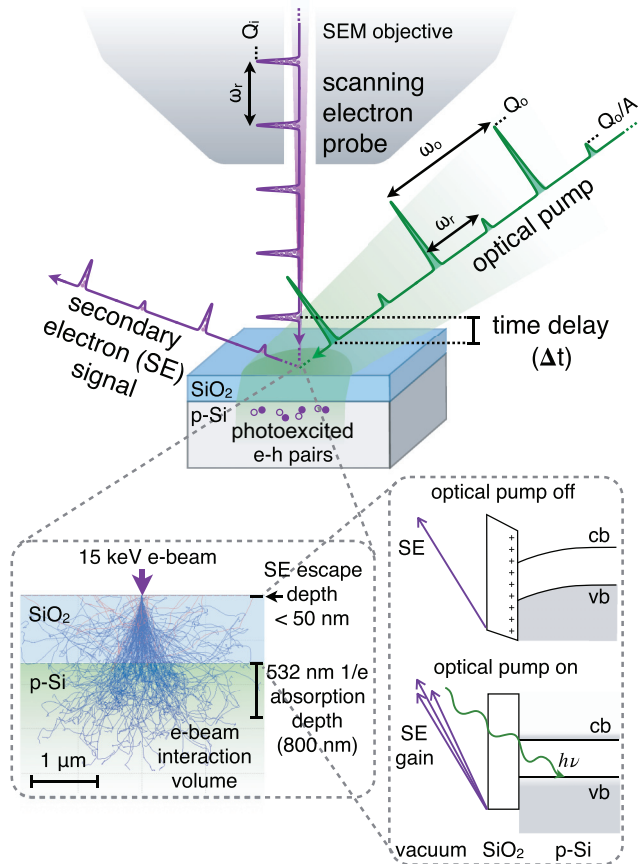
*aatalin@sandia.gov

FIG. 1. Conceptual illustration of SUEM measurement at a buried p-Si/SiO$_2$ interface. The 532 nm pump generates electron-hole (e-h) pairs in the p-Si, spatially separated from the source of SEs near the surface of the oxide. The photoexcited electrons diffuse to the interface where they reduce the local charge and flatten the band bending. This reduces the electric field that limits SE emission from the surface of the 1 μm thick SiO$_2$. The inset shows a Monte Carlo simulation of the 15 keV primary electron beam interaction volume. Although the electron beam interaction extends more than 1 μm below the surface, the SE escape depth is limited to <50 nm.

signal from the MCP anode is capacitively coupled (1 nF) and amplified with a fast transimpedance current amplifier. After the current amplifier, the signal is sent into two lock-in amplifiers, referencing the 2 and 1 MHz Fourier components simultaneously with integration times of 30 and 100 μs, respectively. The 2 MHz signal component accesses the total SE yield as in a typical SEM image while the 1 MHz component accesses the difference in SE emission with and without the pump laser.

Time-resolved SUEM experiments are performed with an accelerating voltage of 15 kV at a working distance of 14 mm. Images are acquired with a pixel dwell time of 156 μs and 367 930 pixels per frame. Pump-probe time delays range from −8 to 8 ns, with positive values indicating that the pump pulse arrives before the electron probe pulse.

p-Si/SiO$_2$ wafers were obtained from UniversityWafer Inc. and used as received. We used the four-point probe method to measure the electronic resistivity $R = 0.02 \, \Omega$ cm,
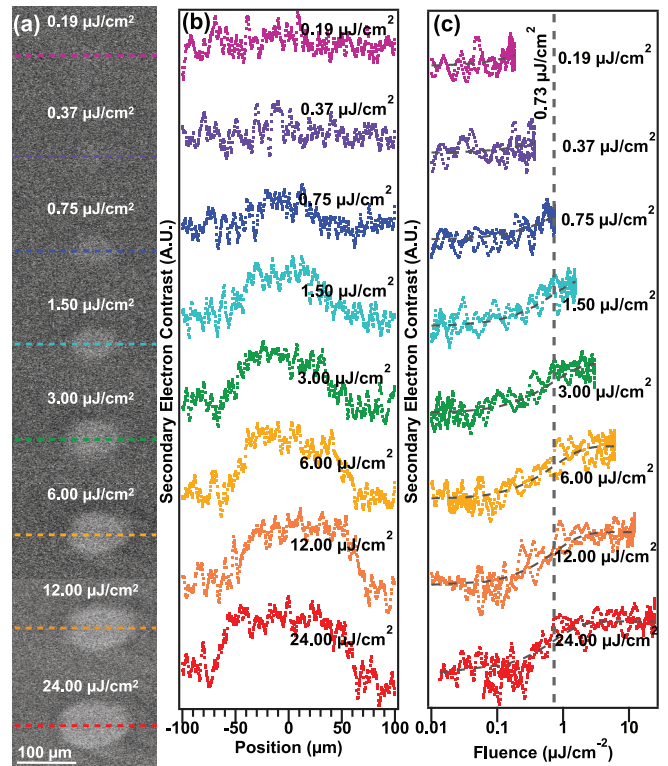

FIG. 2. (a) Fluence dependence of the SUEM photon-electron interaction region upon doubling the pump laser power while maintaining a constant pump-probe time delay of 1.94 ns. The peak fluence of the laser profile is indicated in each image. (b) Horizontal line profiles taken from the SUEM images. The intensities have been shifted but not scaled and the numbers on the plot indicate the peak fluence. (c) Fluence dependence of the signal. The gray dashed lines are fits of the form $C[\, 1 - \exp(-f/f_s)]$ where f is the fluence and f_s is the fitted 1/e from a saturation level of 0.73 μJ cm^{-2}.

which corresponds to a B doping $N_A = 4.2 \times 10^{18}$ cm^{-3}. At the p-Si/SiO$_2$ interface pinning of the Si Fermi level leads to interfacial charge and downward band bending [10] in the Si. The interfacial charge also leads to an electric field across the SiO$_2$, estimated to be 0.2 MV/cm. In this SUEM experiment, the 532 nm pump light is primarily absorbed by the Si, where it excites e-h pairs. These e-h pairs diffuse to the interface and are captured by interfacial traps leading to a reduction of the interfacial charge and thus the electric field across the SiO$_2$. Because SEs are only emitted from the near surface region of the SiO$_2$, with escape depths of <50 nm [11], the SUEM signal occurs from the change in the electric field at the SiO$_2$ surface (Fig. 1). To eliminate possible effects of the probe electrons (only two to three electrons are emitted per pulse [3]), the signal obtained with the laser off is subtracted from the signal obtained with the laser on.

III. FLUENCE DEPENDENCE AND PHOTOSATURATION

Figure 2(a) shows time-resolved SEM images for several pump laser fluences acquired for a pump-probe time delay of 1.94 ns. We observe a bright spot (increased SE emission) that grows in intensity and size as the fluence increases. The fluence dependence of this photon-electron interaction region

(PEIR) [Fig. 2(b)] shows that the signal in the middle of the profile saturates at high fluence. To convert the spatial dependence to intensity dependence for each position, the fluence was calculated from the measured beam profile (see Supplemental Material [12]), and the SE intensity is plotted at that fluence in Fig. 2(c). The pump fluence dependence can be fit as $C[1 - \exp(-f/f_{sat})]$ with a saturating fluence $f_{sat} = 0.73\,\mu\text{J/cm}^2$/pulse or 2×10^{12} photons/cm^2/pulse.

Most of the photoexcited electrons have diffused to the Si/SiO$_2$ interface by the time delay of $t = 1.94$ ns. Accounting for the angle of incidence and refraction of 532 nm light in silicon, an effective absorption depth of $\delta = 870$ nm is found [13] and the minority carrier diffusivity is $D_e = 6\,\text{cm}^2\,\text{s}^{-1}$ [14]. The length an electron will diffuse as a function of pump-probe time delay is $\sqrt{D_e t}$. It follows that most of the electrons will have encountered the interface at time delays greater than T where $T = \delta^2/D_e = 1.3$ ns. Thus, for Fig. 2 where $t > T$ the saturation fluence (and photoexcited electron flux to the interface) can be compared to the interface trap density of $\sim 2 \times 10^{12}$/cm^2 at the band edges for Si(001) with thermal SiO$_2$ [15,16]. This suggests complete compensation of the interfacial charge at the saturating fluence, in which case the electric field across the oxide vanishes.

This photovoltage mechanism explains the SUEM contrast. Indeed, Monte Carlo simulations have shown [11] that the escape probability of SE electrons at a depth z in SiO$_2$ is given by $p(z) = p_0 \exp[-z/\lambda(F)]$ with $\lambda(F) = \lambda_0 \exp(F/F_a)$ where F is the electric field in the SiO$_2$. The initial positive field of 0.2 MV/cm reduces the escape probability; illumination removes this electric field and increases SE emission, in agreement with the experimental observation. Furthermore, the observed $\sim 8\%$ change in signal at saturation is consistent with the above equations (see Supplemental Material [12]). Recent SEM-based measurements of the PV on p-Si with a thin SiO$_2$ layer observed a decreased SE yield at moderate fluence, but an increase yield at high fluence [17]. Dark contrast is absent in our experiment even at low fluence because the SEs originate from the thick oxide instead of the semiconductor.

IV. SPATIOTEMPORAL CARRIER DYNAMICS

The pulsed excitation and detection afforded by SUEM enables the probing of saturation dynamics of the interfacial states, which is not generally accessible to steady state laser experiments because the high laser fluence required to fully populate the short-lived trap states would melt the sample [18]. Figure 3 presents a time series of SUEM images with varying pump-probe time delays. At early times a bright PEIR appears, corresponding to an increase in secondary electron emission of about 8%. The PEIR rapidly expands beyond the beam radius $(1/e^2)$ over the first hundred picoseconds. Figure 3(b) shows the time dependence of the SUEM signal averaged over annular elliptical regions of uniform fluence. The signal increases over a timescale of a few hundred picoseconds. The initial rise time depends strongly on fluence. The signal decay is nonexponential with both short- and long-lived components.

This behavior is consistent with how the surface photovoltage of the Si/SiO$_2$ interface is expected to evolve. The
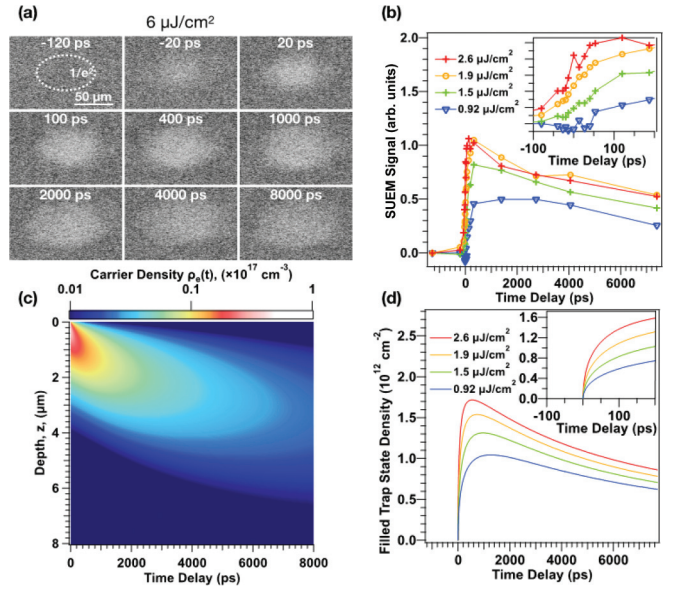

FIG. 3. (a) Time evolution of SUEM signal showing rapid expansion of an elliptical disk. The peak fluence and the beam radius are indicated. (b) SUEM signal in annular regions surrounding the disk as a function of time for various fluences. (c) Model of carrier diffusion in the presence of a saturable sink at the Si/SiO$_2$ interface. (d) Simulated time dependence of trap state density for various fluences.

initial rise time is determined by the number of photoexcited electrons and how quickly they diffuse to charge traps at the interface. As the traps are occupied, the interfacial potential changes and eventually the interface can no longer accept more electrons. This leads to the observed saturation in the SUEM signal. At later times, holes in the Si recombine with the electrons at the interface causing the SUEM signal to decrease. The recombination process is slower than the filling process because holes diffuse slower than electrons in Si and are initially repelled from the interface because of band bending [19]. To quantitively compare this simple picture with experiment, a simplified one-dimensional diffusion and trapping model was developed (see Fig. 3(c) and the Supplemental Material [12]). Photoexcited conduction band electrons $\rho_e(t, z)$ are rapidly injected into the system at time zero to prepare the initial carrier density of

$$\rho_e(0, z) = \frac{f}{h\nu\delta} \exp(-z/\delta). \tag{1}$$

The electron density evolves according to the diffusion equation,

$$\frac{\partial \rho_e(t, z)}{\partial t} = D_e \frac{\partial^2 \rho_e(t, z)}{\partial z^2}. \tag{2}$$

We assume that the interface is a saturable sink for these diffusing electrons and provides a constraint that slows the rate of trapping as the number of occupied traps approaches saturation, ρ_{sat}. Furthermore, the recombination rate of traps is assumed to be superlinear with the number of occupied traps because the barrier to recombination with holes is diminished as the interfacial charge is compensated [19,20]. The result of this model for the occupied trap density is shown in

Fig. 3(d), assuming previous estimates for D_e (6 cm^2 s^{-1}) and ρ_{sat} (2×10^{12}/cm^2), and treating the recombination rate as an adjustable parameter. The number of occupied traps (and thus photovoltage) in the model reproduces the observed evolution of the SUEM signal, increasing our confidence in the interpretation of the SUEM signal originating from a photovoltage effect.

V. CONCLUSION

Nondestructive techniques for measuring dynamics and material parameters of buried interfaces in topographically complex samples is highly sought after in fields such as piezoelectric sensors, solid-electrolyte battery interfaces [21], photovoltaics [22], and multilayer microelectronics [23]. The SUEM technique is able to remotely probe buried interfaces with picosecond time resolution. SUEM is sensitive to the trapping of the minority carriers in p-Si at the SiO$_2$ interface. In the regime of high excitation rate, photoexcited carriers can saturate the available trap states on timescales as short as a few picoseconds. The versatility of the technique is demonstrated by also probing the dynamics over nanoseconds where

thermally activated trap recombination dominates. Our results reveal a previously unidentified SUEM contrast mechanism, thus expanding the scope of systems and scientific questions which can be addressed using this technique.

[1] K. C. Collins, A. M. Armstrong, A. A. Allerman, G. Vizkelethy, S. B. Van Deusen, F. Léonard, and A. A. Talin, J. Appl. Phys. **122**, 235705 (2017).

[2] A. A. Talin, R. S. Williams, B. A. Morgan, K. M. Ring, and K. L. Kavanagh, Phys. Rev. B **49**, 16474 (1994).

[3] D.-S. Yang, O. F. Mohammed, and A. H. Zewail, Proc. Natl. Acad. Sci. USA **107**, 14993 (2010).

[4] O. F. Mohammed, D.-S. Yang, S. K. Pal, and A. H. Zewail, J. Am. Chem. Soc. **133**, 7708 (2011).

[5] D.-S. Yang, B. Liao, and O. F. Mohammed, MRS Bull. **43**, 491 (2018).

[6] E. Najafi, T. D. Scarborough, J. Tang, and A. H. Zewail, Science **347**, 164 (2015).

[7] E. Najafi, V. Ivanov, A. Zewail, and M. Bernardi, Nat. Commun. **8**, 15177 (2017).

[8] B. Liao, E. Najafi, H. Li, A. J. Minnich, and A. H. Zewail, Nat. Nanotechnol. **12**, 871 (2017).

[9] B. Liao, H. Zhao, E. Najafi, Y. Xiaodong, H. Tian, J. Tice, A. J. Minnich, H. Wang, and A. H. Zewail, Nano Lett. **17**, 3675 (2017).

[10] L. Kronik and Y. Shapira, Surf. Sci. Rep. **37**, 1 (1999).

[11] E. Schreiber and H.-J. Fitting, J. Electron Spectrosc. **124**, 25 (2002).

[12] See Supplemental Material at http://link.aps.org/supplemental/10.1103/PhysRevB.104.L161303 for additional information on fluence calculation, signal change at saturation, and on the one-dimensional model.

[13] E. D. Palik, *Handbook of Optical Constants of Solids* (Academic Press, New York, 1985).

[14] W. R. Thurber, R. L. Mattis, Y. M. Liu, and J. J. Filliben, J. Electrochem. Soc. **127**, 1807 (1980).

[15] D. K. Schroder, *Semiconductor Material and Device Characterization* (John Wiley and Sons, New York, 2006), p. 349.

[16] M. Takihara, T. Takahashi, and T. Ujihara, Appl. Phys. Lett. **93**, 021902 (2008).

[17] Y. Li, U. Choudhry, J. Ranasinghe, A. Ackerman, and B. Liao, J. Phys. Chem. A **124**, 5246 (2020).

[18] O. B. Aphek, L. Kronik, M. Leibovitch, and Y. Shapira, Surf. Sci. **409**, 485 (1998).

[19] W. Widdra, D. Bröcker, T. Gießel, I. V. Hertel, W. Kruuger, A. Liero, F. Noack, V. Petrov, D. Pop, P. M. Schmidt, and R. Weber, Surf. Sci. **543**, 87 (2003).

[20] B. F. Spencer, D. M. Graham, S. J. O. Hardman, E. A. Seddon, M. J. Cliffe, K. L. Syres, A. G. Thomas, S. K. Stubbs, F. Sirotti, M. G. Silly, P. F. Kirkham, A. R. Kumarasinghe, G. J. Hirst, A. J. Moss, S. F. Hill, D. A. Shaw, S Chattopadhyay, and W. R. Flavell, Phys. Rev. B **88**, 195301 (2013).

[21] M. Golozar, A. Paolella, H. Demers, S. Bessette, M. Lagacé, P. Bouchard, A. Guerfi, R. Gauvin, and K. Zaghib, Commun. Chem. **2**, 131 (2019).

[22] H. Zhou, Q. Chen, G. Li, S. Luo, T.-b. Song, H.-S. Duan, Z. Hong, J. You, Y. Liu, and Y. Yang, Science **345**, 542 (2014).

[23] H. Atsufumi, Y. Yamamoto, M. A. Benedict, and A. J. Vick, Nat. Commun. **7**, 12701 (2016).